Original Research

Identification of candidate biomarker *EMP3* and its prognostic potential in clear cell renal cell carcinoma

Qingyang Lv[1,2,†], Wen Xiao[1,2,†], Zhiyong Xiong[1,2,†], Jian Shi[1,2], Daojia Miao[1,2], Xiangui Meng[1,2], Hongwei Yuan[1,2], Hongmei Yang[3,*], Xiaoping Zhang[1,2,*]

[1]*Department of Urology, Union Hospital, Tongji Medical College, Huazhong University of Science and Technology, 430022 Wuhan, Hubei, China,* [2]*Institute of Urology, Union Hospital, Tongji Medical College, Huazhong University of Science and Technology, 430022 Wuhan, Hubei, China,* [3]*Department of Pathogenic Biology, School of Basic Medicine, Huazhong University of Science and Technology, 430022 Wuhan, Hubei, China*

TABLE OF CONTENTS

Submitted: 1 October 2021 Revised: 29 October 2021 Accepted: 29 October 2021 Published: 30 November 2021

1. Abstract

Background: Clear cell renal cell carcinoma (ccRCC) is considered the second most common urogenital tract carcinoma, plaguing patients worldwide due to its high incidence and resistance to treatment. Thus, it is urgent to screen new biomarkers and decipher their molecular mechanisms to support early clinical diagnosis and targeted therapy of ccRCC. It is reported that epithelial membrane protein 3 (*EMP3*) acts as a tumor-promoting or suppressing factor in a variety of malignant tumors, but its relationship with ccRCC remains to be explored. **Methods**: The Cancer Genome Atlas (TCGA) and Oncomine database were utilized to screen the differentially expressed genes in ccRCC. Western blot and qPCR were used to verify the expression of our subject of interest, *EMP3* in ccRCC tissues and cell lines. Next, a series of functional experiments were conducted to explore the biological functions of *EMP3* in tumor cells, including cell counting kit-8, transwell, wound healing assays, Oil red O staining and triglyceride determination. Western blotting was used to explore the potential mechanism of *EMP3* induced ccRCC deterioration. Finally, the TIMER2.0 database was used to explore the effect of *EMP3* on tumor immune infiltration and its relationship with multiple immune checkpoints. **Results**: In this study, we uncovered that *EMP3* was more prominently expressed in ccRCC and its expression level had a significant positive correlation with the clinical stage and histopathological grade of tumor patients. Based on the TCGA database, the Receiver operating characteristic (ROC) curves showed that *EMP3* could be potentially utilized as a specific biomarker in diagnosing ccRCC patients. Meanwhile, six independent prognostic factors were determined and integrated into our nomogram, with an OS concordance index (C-index) of 0.760 (95% CI: 0.689–0.831). Furthermore, *in vitro* depletion of *EMP3* could alleviate the proliferation, migration, invasion, and lipid storage in ccRCC cells. Mechanistically, *EMP3* was shown to enhance the malignant potential of tumor cells by promoting epithelial-mesenchymal transition (EMT) and lipid accumulation. In addition, the expression of *EMP3* was closely related to the infiltration of a variety of immune cells, and was positively related to PD-L1, suggesting that it may be a tight connection with tumor immune escape. **Conclusions**: Our results revealed that *EMP3* might be a candidate biomarker and independent prognostic indicator, and related to EMT process, lipid accumulation, as well as immune infiltration in ccRCC. Targeted *EMP3* therapy might be a promising and effective treatment strategy for ccRCC patients.

2. Introduction

Renal cell carcinoma originating from renal tubular epithelium is a solid malignant tumor and ranks 16th among all malignancies worldwide. There were approximately 430,000 new diagnostic cases and 179,000 estimated deaths resulting from kidney tumors in 2020 all over the world [1]. Among the histological subtypes of renal cancer, ccRCC has proven to be the most common tubule-derived malignancy, accounting for about 80%–90% [2, 3]. Thanks to imaging technology enhancement, the early detection rate of ccRCC patients has improved significantly over the years. Nevertheless, the clinical outcomes of patients with ccRCC tumor progression or distant metastasis remain extremely poor, accompanied by a 5-year survival rate of only 10%–20% [3, 4]. This could be due to the significant tumor heterogeneity in ccRCC, resulting in over 75% of advanced patients not responding to first-line antiangiogenic drugs [5]. Consequently, it is important to seek novel and effective biomarkers to guide clinicians to choose more effective drugs and formulate more robust treatment strategies.

Epithelial membrane protein 3 (*EMP3*), a mesenchymal characteristic gene also called YMP, belongs to the well-conserved peripheral myelin protein 22 (PMP22) family of proteins, which are involved in cell-to-cell adhesion and cell survival [6–8]. *EMP3* contains four transmembrane domains and two N-linked glycosylation sites and is located on chromosome 19q13.3 region and was originally regarded as a tumor-suppressive gene in multiple malignancies, especially in the central nervous system (CNS) tumors [9]. The down-regulated *EMP3* expression in these tumors greatly relates to various clinical features and heralds a worse prognosis [10–12]. Abnormally increased promoter methylation of *EMP3* was regarded as one of the main causes for its transcriptional silencing [13]. On the other hand, there is growing evidence showing that *EMP3* could be involved in driving tumorigenesis and cancer progression, acting as an oncogene related to the EMT process in certain cancer types. Han *et al*. [14] found that *EMP3* overexpression could regulate epithelial-mesenchymal transition and indicate metastasis or progression of gastric cancer. It has been clarified that *EMP3* has a functional crosstalk between the well-known oncogene ErbB2 in upper urinary tract urothelial carcinoma and that the overexpression of *EMP3* significantly facilitated proliferation and migration of cancer cells [15]. However, the gene expression status and biological functions of *EMP3* in ccRCC remain elusive.

Herein, we compared the expression level of *EMP3* in ccRCC and paired healthy tissues obtained from the TCGA database. Next, the clinicopathological features, survival significance and diagnostic value of *EMP3* were investigated in ccRCC patients by stratifying them into several subgroups for further analysis. In addition to bioinformatics analysis, clinical samples and cellular models were examined to confirm the differential expression and explore the role of *EMP3* in the deterioration of ccRCC. Our study indicated that high *EMP3* expression could predict a poor prognosis and acted as an oncogene by activating the EMT signaling pathway in ccRCC. Thus, our analysis high-

lighted the importance of *EMP3* as an effective diagnostic tool and potent therapeutic target in ccRCC patients.

3. Materials and methods

3.1 Bioinformatics analysis

The Cancer Genome Atlas (TCGA) program is one of the largest tumor databases in the world, containing clinical data and gene expression profiles of thousands of patients with 33 different cancer types [16, 17]. The RNA-seq expression files and relevant clinicopathological and survival data of TCGA-KIRC patients were acquired from the University of California, Santa Cruz (UCSC) Xena browser (https://xenabrowser.net). There were 533 ccRCC samples and 72 paired normal tissues included in this database. Oncomine database (http://www.oncomine.org/) is a gene-centric analysis platform by integrating multiple datasets, and is widely used for gene differential expression analysis [18]. Similarly, the Oncomine database was utilized to compare the EMPs family expression level, including *EMP1*, *EMP2* and *EMP3*. *EMP3* was chosen as our research object, and its differential expression was further confirmed in four subsets of the Oncomine website.

The ROC curve was utilized to measure the diagnostic value of *EMP3* in people suffering from ccRCC. According to the median expression of *EMP3*, we analyzed the survival data of ccRCC patients. Then we established a nomogram model by grouping them into two groups (high versus low) and performed Cox-regression analysis to illustrate the prognostic role of *EMP3* in ccRCC. The calibration curves of 1-, 3-, and 5-years were drawn to evaluate the performance of the nomogram. The ArrayExpress database, which afflicted to The European Bioinformatics Institute (EMBL-EBI), collected a large amount of chip microarray data for scientific research personnel to explore [19]. The E-MTAB-1980 cohort was used to verify the prognostic significance of *EMP3* in ccRCC.

Gene set enrichment analysis (GSEA) and gene expression correlation analysis were implemented to bring us some clues to uncover the potential biological mechanism behind *EMP3* in ccRCC. The false discovery rate (FDR) <0.25 was considered to have sufficient significance to eliminate inadequate signal pathways. The permutations for each phenotype were carried out 1000 times ($p < 0.05$).

3.2 Clinical patient samples

The 28 paired clinical samples were all from ccRCC patients who underwent surgical treatment at the Department of Urology, Union Hospital Affiliated to Tongji Medical College (Wuhan, China) from 2016 to 2021. They had never received preoperative chemotherapy or radiotherapy and informed consent was signed. After the tumor tissues and matched para-carcinoma renal tissues were isolated, both of them were frozen in liquid nitrogen quickly to prevent total RNA and protein degradation. Part of collected samples were immersed in 10% formalin to fix. According to the Declaration of Helsinki, the Ethics Committee of Huazhong University of Science and Technology (Wuhan, China) approved our experimental protocol.

3.3 Cell lines and cell culture

Normal human renal epithelial cell lines 293 and RCC cell lines (A498, 786-O, CAKI-1, ACHN and OSRC-2) in our study were purchased from the cell bank of American Type Culture Collection (Manassas, VA, USA). All the cell lines except 786-O were cultivated in high-glucose DMEM supplemented with 10% fetal bovine serum (FBS, Gibco; Thermo Fisher Scientific, Waltham, MA, USA) and 1% penicillin-streptomycin (Gibco; Thermo Fisher Scientific; Waltham, MA, USA), and then cultured at the atmosphere of 5% CO_2 in 37 °C constant temperature incubator. 786-O was cultured separately with RPMI 1640 medium supplied with the above serum and penicillin-streptomycin.

3.4 RNA extraction and qRT-PCR

According to the manufacturer's protocol, the clinical tissue specimens were prepared by grinding while cells were collected before mixing with the TRIzol reagent (Thermo Fisher Scientific; Waltham, MA, USA) to isolate and extract total RNA from tissues and cells, respectively. The NanoDrop 2000 spectrophotometer (Thermo Fisher Scientific; Rockford, IL, USA) was then utilized to detect its purity and concentration. Reverse transcription method was conducted to amplify the corresponding mRNA we need. All the qPCR were performed using the Step one plus (ABI; Thermo Fisher Scientific, Rockford, IL, USA) platform using the SYBR Green mix (Thermo Fisher, Massachusetts, USA). Primers for gene *EMP3* were designed and purchased from TsingKe (Tsingke Biological Technology; Wuhan, China) and are listed as follows:

EMP3

Forward primer
5′-CCTGAATCTCTGGTACGACTGC-3′;
Reverse primer
5′-GCCATTCTCGCTGACATTACTG-3′.

β-actin

Forward primer
5′-CTCGCCTTTGCCGATCC-3′;
Reverse primer
5′-TTCTCCATGTCGTCCCAGTT-3′.

3.5 Immunohistochemistry (IHC)

The ccRCC tumor tissues and adjacent normal renal tissues were fixed with 10% formalin and embedded in paraffin. Next, the wax blocks were cut into slices about 5 μm thick. Subsequently, after deparaffinization and hydration, the slices were incubated with primary mouse anti-*EMP3* monoclonal antibody (Santa Cruz, sc-81797, 1:200) overnight in a refrigerator at 4 °C. The tissue sections were then incubated with secondary antibody at room temperature and colored using 3,3-N-Diaminobenzidine Tetrahy-

drochloride (DAB). Finally, hematoxylin was used to counterstain the tissue cells, and the samples were observed under a microscope.

3.6 Western blot

Collected clinical tissues and cells were lysed with a series of proteolytic agents, including RIPA lysis buffer (Beyotime Biotechnology; Haimen, China), phenylmethylsulfonyl fluoride (PMSF) and protease inhibitor cocktail (Roche Diagnostics; Indianapolis, IN, USA). After centrifugation to remove excess residue, the protein concentration was measured using the bicinchoninic acid assay (Thermo Fisher Scientific; Waltham, MA, USA) at a wavelength of 562 nm. The total protein extracts were added to 10% SDS-PAGE wells, then concentrated, separated and transferred onto the PVDF membrane (Roche Diagnostics; Indianapolis, IN, USA). The membranes were repeatedly washed three times with PBST after being blocked by defatted milk for at least one hour. According to the indicators of gel electrophoresis markers, the membranes were cut into the desired strips for further processing. The bands of interest were incubated with the primary antibody at 4 °C for at least 12 hours, washed again and incubated with the secondary antibody at room temperature for two hours, and then photographed. Antibodies used in the study were as follows: anti-*EMP3* (Santa Cruz, sc-81797, 1:200), anti-β-actin (Proteintech, 20536-1-AP, 1:1000), anti-E-cadherin (Abclonal, A18135, 1:1000), anti-N-cadherin (Abclonal, A19083, 1:1000), anti-VIM (Abclonal, A19607, 1:1000), and anti-SNAIL (Abclonal, A11794, 1:1000).

3.7 Transient transfection

786-O and A498 cell lines were selected for *in vitro* experiments. The sgRNAs targeting *EMP3* were designed using the synthego website (https://www.synthego.com) and utilized for knockdown experiments in the above-mentioned cell lines. The cell density in the 6-well plate was maintained at 50%–60% confluence, and Lipofectamine 3000 (Invitrogen, Carlsbad, CA, USA) was mixed with the sgRNAs according to the manufacturer's instructions to carry out the transfection procedure. The efficiency of *EMP3* knockdown was verified by Western blot and qPCR after 48 h. The sgRNA sequences for *EMP3* designed by the CRISPR-editing platform are as follows (**Supplementary Fig. 1**):

5′-CAGGGAGAGUCCACCAGGAC-3′ (1#);
5′-UCUGUCCAUCCCAGUCCUGG-3′ (2#);
5′-UUUCCCAGGGAGAGUCCACC-3′ (3#).

3.8 Cell proliferation assay

For cell proliferation assays, 2×10^3 cells from each group (sg-*EMP3* and CON) were seeded in a 96-well plate. Cell counting kit-8 (Bio-Rad Laboratories, Hercules, CA, USA) was diluted to 10% using DMEM and added to the wells to measure the OD value at 450 nm using a microplate reader.

3.9 Wound healing assays

The complete medium for culturing tumor cells in six-well plates was replaced with a serum-free medium. Then a 200 μL pipette tip was used to draw a straight wound, and the wells were washed three times to remove cell debris. The scratch images at 0 h and 24 h were taken and recorded under a microscope (Olympus; Tokyo, Japan) at 100 $\times$ magnification by selecting three random fields of view.

3.10 Transwell assays

In the migration assays, we inoculated 2×10^4 cells into the upper chamber of a 24-well transwell chamber (Costar, 3422; Corning Incorporated, NY, USA) and incubated them in a serum-free medium for 24 hours. At the same time, 600 μL complete medium (supplemented with 10% FBS) was added to the bottom of the chamber. The chambers were soaked in 20% methanol, fixed for 10 minutes, and then stained in 0.5% crystal violet solution for 15 minutes. After washing several times, the cells on the upper surface were gently wiped off with a cotton swab, and the bottom surface of the chambers was photographed and counted under a 200 $\times$ light microscope.

Similarly, in the invasion assays, 8×10^4 cells were seeded into the upper chamber containing a non-serum medium pre-paved with Matrigel (Thermo Fisher Scientific; Waltham, MA, USA). Simultaneously, 600 μL complete medium supplemented with 10% FBS was added under the chamber to form a nutrient induction trend. After 24 h of co-incubation in a humid environment, the invasive cells were washed, fixed and stained, as mentioned before. Subsequently, five random fields were imaged to count the number of cells under a light microscope (Olympus; Tokyo, Japan). This experiment was independently conducted more than three times.

3.11 Oil red O staining and triglyceride determination

The cells were cultured in a six-well plate to about 30% confluence, washed with PBS and fixed with 10% formaldehyde for at least 20 minutes. After washing again, Oil Red O (Wuhan Service Biotechnology Company; Wuhan, Hubei, China) was added to each well for 30 minutes. According to the manufacturer's instructions, a triglyceride determination kit (Nanjing Jiancheng Institute of Bioengineering; Nanjing, Jiangsu, China) was used to detect triglyceride content in cancer cells.

3.12 TIMER 2.0 database

The "Gene Module" in the TIMER 2.0 database (http://timer.cistrome.org/) was explored to analyze the relationship between *EMP3* and tumor immune cell infiltration [20]. Furthermore, "Gene_Corr Module" was a gene co-expression model constructed based on the expression data in the TCGA database. It can be used to view the

Spearman's expression correlation between target genes and immune checkpoints.

3.13 Statistical analysis

SPSS statistics version 25.0 (version 21.0, IBM Corp, Chicago, IL, USA) and GraphPad Prism (version 6.0, GraphPad Software Inc, San Diego, CA, USA) were employed for all data analysis. Unpaired or paired Student's *t*-test was utilized to distinguish the difference between two groups. Furthermore, differences among multiple groups were evaluated by one-way analysis of variance (ANOVA; #). The Kaplan-Meier curve analysis and nomogram were drawn to analyze the survival probability of ccRCC patients according to the expression level of *EMP3*. The diagnostic value of *EMP3* expression level was clarified using the receiver operator characteristic (ROC) curve. The prognostic role of *EMP3* was investigated using the Cox proportional hazard regression and displayed using forest plots. Statistical data were presented as the mean ± standard deviation (SD). The data differences were considered statistically significant when the calculated p-value < 0.05.

4. Results

4.1 *EMP3* is highly expressed in ccRCC via database analysis

The EMP family has been reported to be related to various pathological processes; however, its role in ccRCC is not clear. To investigate the expression of EMP family members in ccRCC, the TCGA-KIRC dataset was analyzed and revealed that *EMP3* mRNA expression in ccRCC was significantly elevated compared to corresponding noncancerous tissue samples (Fig. 1A,B). Furthermore, four gene expression datasets were downloaded from Oncomine for further validation; *EMP3* was found to be abnormally upregulated in ccRCC (Fig. 1C). Based on these findings, we sought to further investigate the role of *EMP3* in ccRCC.

4.2 Highly expressed *EMP3* is closely related to multiple clinicopathological parameters in ccRCC patients

To explore the difference in *EMP3* mRNA expression among clinical characteristics of ccRCC patients, including sex, age, tumor grade and TNM stage, data extracted from the TCGA database was mined and compared (Table 1). *EMP3* expression levels in tumors and normal tissues from the TCGA-KIRC database were compared using Student's *t*-test (Fig. 2A,B). The results showed that *EMP3* expression was elevated in paired or unpaired tissue samples of ccRCC. Further subgroup analysis revealed that high expression of *EMP3* was positively associated with male (Fig. 2C), advanced T stage (Fig. 2D), TNM stage (Fig. 2E) and histological grade (Fig. 2F). The comparison of grouped expression levels made it easier to obtain the relationship between clinicopathological features and *EMP3* expression in ccRCC.

Table 1. Correlation between *EMP3* mRNA expression and clinicopathological parameters of ccRCC patients.

Parameter	number	EMP3 mRNA expression		*p* value
		High (n = 258)	Low (n = 259)	
Age(years)				
≤60	257	123	134	
>60	260	135	125	0.356
Gender				
Female	181	80	101	
Male	336	178	158	0.057
T stage				
T1 + T2	332	142	190	
T3 + T4	185	116	69	0.000
N stage				
N0 + NX	503	245	258	
N1	14	13	1	0.001
M stage				
M0 + MX	441	205	236	
M1	76	53	23	0.000
TNM stage				
I + II	314	127	187	
III + IV	203	131	72	0.000
Grade				
G1 + G2	239	94	145	
G3 + G4	278	164	114	0.000

EMP3, Epithelial membrane protein 3; TNM, T, tumor; N, regional lymph node; M, metastasis.

4.3 *EMP3* is a biomarker of ccRCC with diagnostic value

Parameters, including metastasis, tumor stage, histological grade, TNM stage and disease recurrence, are important factors that influence treatment selection during clinical practice. All included ccRCC patients (n = 533) were stratified according to the above parameters. *EMP3* expression yielded good predictive performance in differentiating between ccRCC and healthy samples with an area under the curve (AUC) of 0.9356 (95% CI: 0.9063 to 0.9649, $p < 0.0001$) (Fig. 3A). The AUC value of paired samples was 0.9418 (95% CI: 0.9008 to 0.9829, $p < 0.0001$) (Fig. 3B). After stratification, the AUCs for *EMP3* expression in differentiating between (T1 + T2) vs. (T3 + T4), (M0 + MX) vs. (M1), (G1 + G2) vs. (G3 + G4), TNM (I + II) vs. (III + IV) and nonrecurrence vs. recurrence were 0.6288, 0.6577, 0.6602, 0.6580 and 0.6671, respectively. Statistically significant differences were observed in all groups during subgroup analysis (Fig. 3C–G, $p < 0.0001$). Based on these observations, we concluded that *EMP3* could be used as a potential diagnostic biomarker for ccRCC patients.

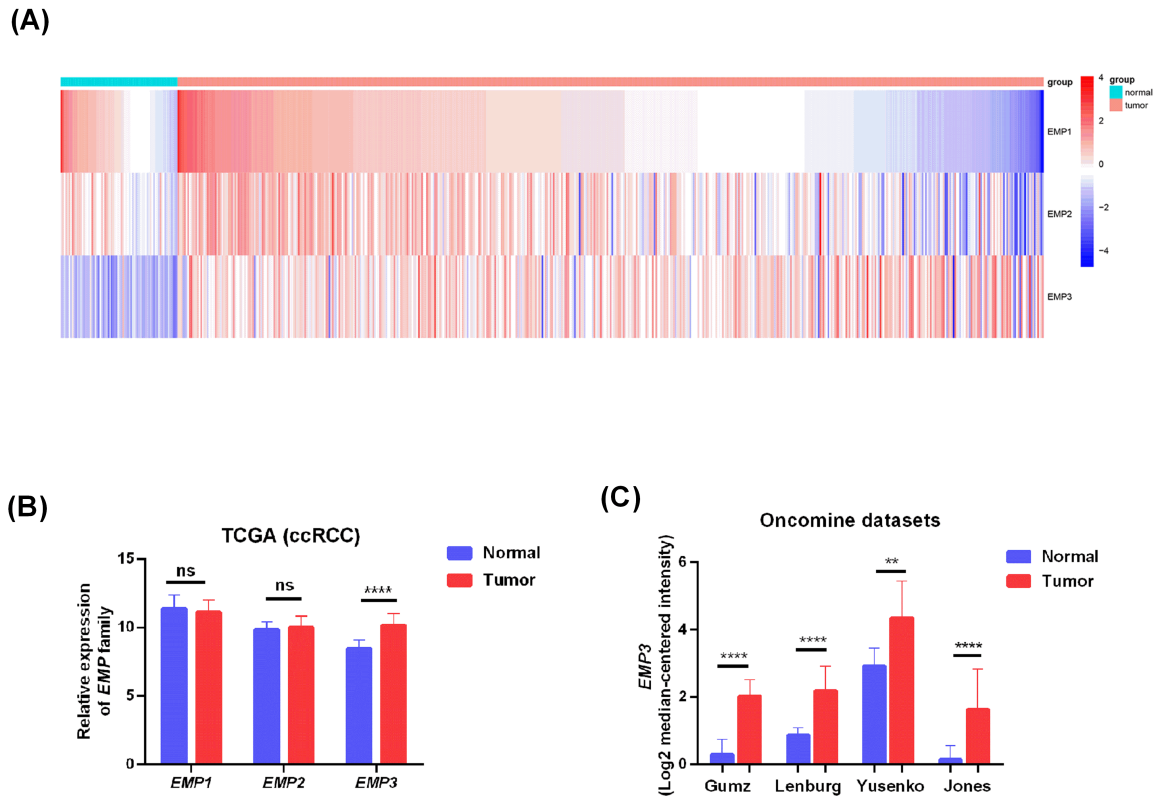

Fig. 1. *EMP3* is highly expressed in ccRCC via database analysis. (A) Heat map depicting EMPs expression in TCGA-KIRC microarray datasets (n = 605). (B) Relative EMPs mRNA expression in TCGA-KIRC. (C) *EMP3* mRNA expression in four Oncomine subsets, including Jones, Gumz, Yusenko and Lenburg renal statistics. $^{**}p < 0.01$, $^{***}p < 0.001$, and $^{****}p < 0.0001$.

4.4 *EMP3* is a biomarker of ccRCC with prognostic significance

After grouping the patients, Kaplan-Meier (KM) analysis was conducted to assess the prognostic value of *EMP3* in terms of overall survival. Higher *EMP3* expression correlated with shorter OS in ccRCC patients (Fig. 4A, **Supplementary Fig. 2**). In order to verify the prognostic significance of *EMP3* in ccRCC, another database ArrayExpress (E-MTAB-1980) was explored and a consistent conclusion was obtained ($p = 0.0115$, **Supplementary Fig. 3**). Univariate and multivariate analyses showed that dysregulated *EMP3* expression could predict poor prognosis of ccRCC (Fig. 4B). Finally, we established a clinical prediction model based on *EMP3* expression and other prognostic parameters screened by the multivariate Cox analysis. As shown in Fig. 4C, all independent predictors of OS including age (HR, 1.672; $p = 0.001$), T stage (HR, 1.568; $p = 0.014$), N stage (HR, 1.938; $p = 0.049$), M stage (HR, 2.749; $p = 0.000$), tumor grade (HR, 1.653; $p = 0.007$) and *EMP3* expression level (HR, 1.511; $p = 0.013$), were integrated in a prognostic model to individually predict survival of ccRCC patients. The AUCs of overall survival of ccRCC patients at 1-, 3- and 5-years were respectively estimated as 0.6516, 0.6324 and 0.6229. To assess the accuracy of the prediction model, the 1-, 3- and 5-years calibration plots were created to display the degree of concordance between observed and predicted survival outcomes. The calibration plots showed optimal agreement with a concordance index of 0.760 (95% CI: 0.689–0.831), exhibiting the good predictive power of our model (Fig. 4E). In conclusion, our research findings suggested that *EMP3* is a robust biological marker for predicting prognosis in ccRCC patients.

4.5 *EMP3* is significantly upregulated in ccRCC cell lines and tissues

To further validate high *EMP3* expression in ccRCC, we analyzed its expression in ccRCC cell lines and tissues. Consistent with our *in silico* analysis findings, *EMP3* expression was significantly increased in ccRCC cell lines compared to normal human renal epithelium cell line 293 (Fig. 5A,B). Consistent results were obtained in ccRCC cell lines; both *EMP3* mRNA and protein expression in tumor tissues were abnormally upregulated compared with neighboring normal tissues (Fig. 5C,D). In addition, immunohistochemistry confirmed high *EMP3* protein levels in ccRCC tissue specimens (Fig. 5E). Taken together, by integrating bioinformatics and experimental analyses, we further substantiated that *EMP3* was upregulated in ccRCC.

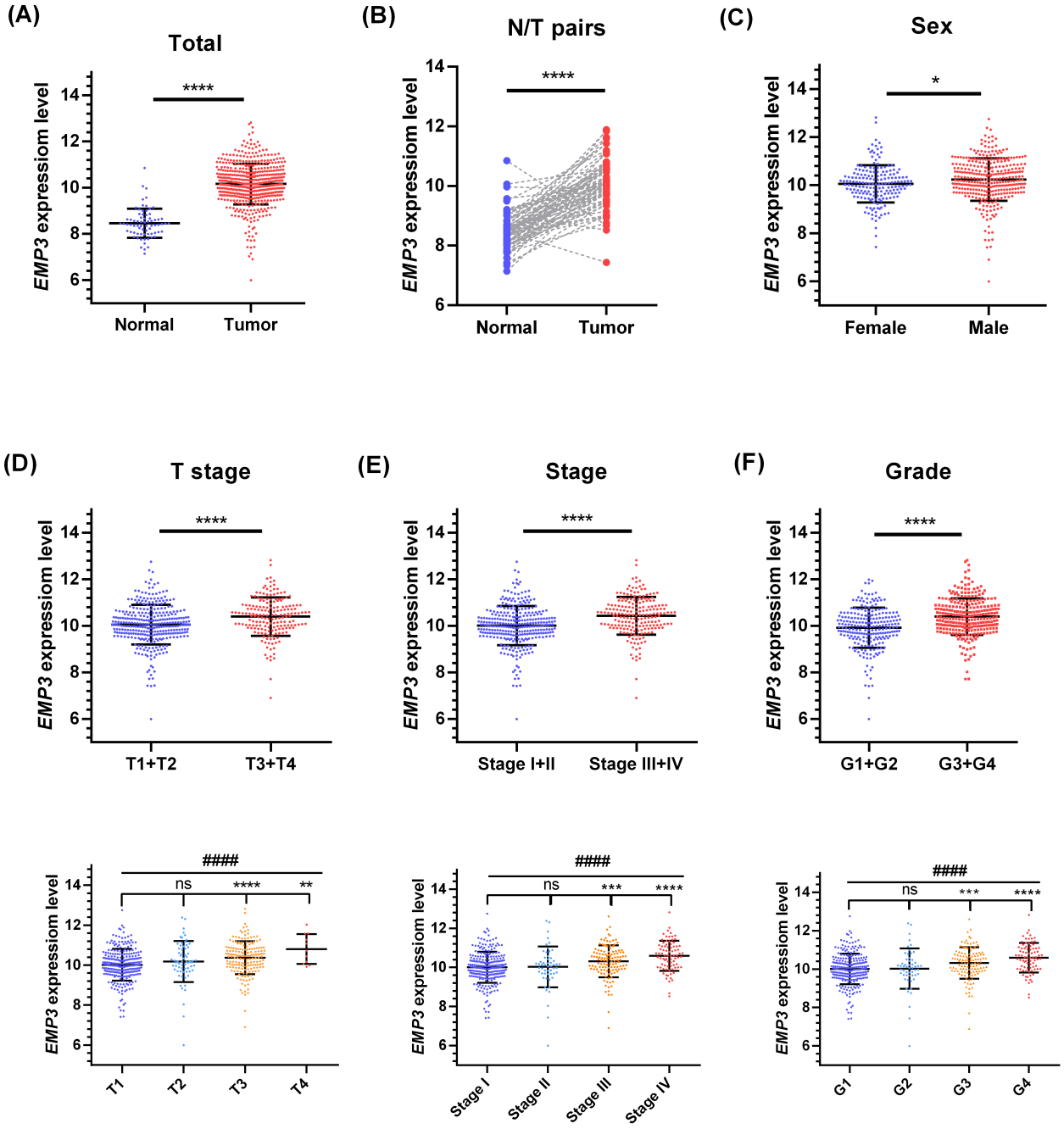

Fig. 2. Highly expressed *EMP3* is closely related to multiple clinicopathological parameters in ccRCC patients. The files of *EMP3* mRNA expression level and ccRCC patient's clinical information were downloaded from TCGA-KIRC datasets and analyzed further in the subgroups: (A) total samples, tumor vs normal. (B) Paired samples, tumor vs normal. (C) Gender. (D) Tumor stage. (E) TNM stage. (F) Pathological grade. Statistical data are presented as the means ± standard deviation. *$p < 0.05$, **$p < 0.01$ ***$p < 0.001$, and ****$p < 0.0001$, #(ANOVA).

4.6 Knockdown of *EMP3* inhibits the malignant phenotypes of ccRCC *in vitro*

Studies have shown that the dysregulation of *EMP3* expression played an oncogenic role in various malignant tumors. To substantiate that the biological functions of *EMP3* in ccRCC, we successfully knocked down *EMP3* in both ccRCC cell lines (A498 and 786-O) by plasmid transfection and then quantified *EMP3* protein and mRNA levels (Fig. 6A,B). Subsequently, we explored the functional impact of *EMP3* knockdown on the two ccRCC cell lines. As shown in Fig. 6C,D, the cell proliferation rate was significantly decreased in the sg-*EMP3* group compared with the NC groups. Moreover, silencing *EMP3* significantly reduced the number of cancer cells stained on the bottom of the transwell (Fig. 6E,F). Similarly, after 24 hours of serum-free culture, the migration ability of tumor cells in

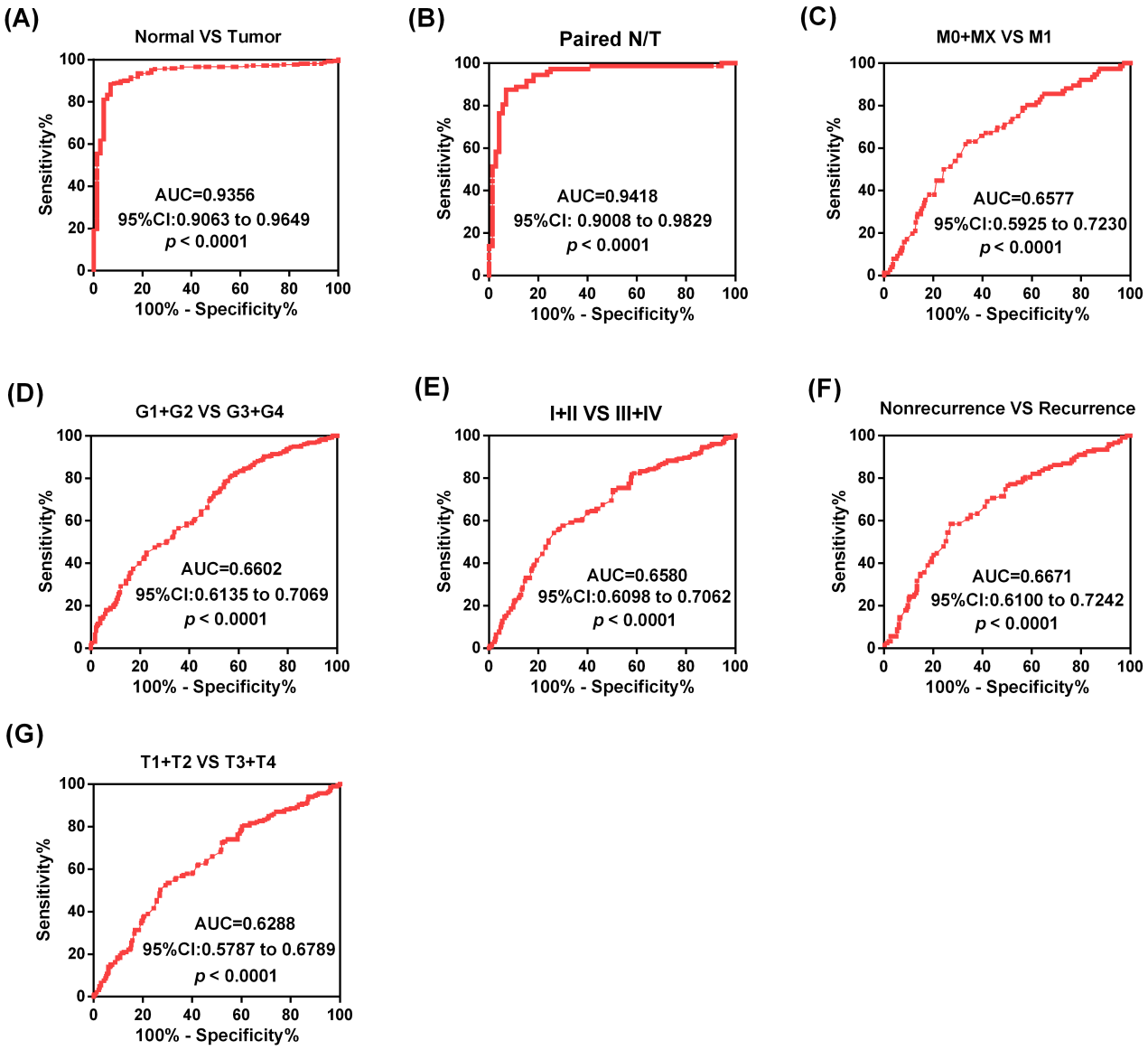

Fig. 3. *EMP3* is a biomarker of ccRCC with diagnostic value. (A) ROC curve analysis of *EMP3* expression indicates that it could discriminate ccRCC and para-cancer tissues in an effective manner. Similar results present in other subgroups. (B) Paired samples. (C) Distant metastasis. (D) Pathological grade. (E) TNM stage. (F) Recurrence status. (G) Tumor stage.

the knockdown *EMP3* group was significantly weakened compared with the control group (Fig. 6G,H). Taken together, it can be inferred that *EMP3* acts as an oncogene in ccRCC by promoting the proliferation, migration and invasion of cancer cells.

4.7 *EMP3* affects the malignant phenotypes of ccRCC by promoting EMT and lipid accumulation

To determine the regulatory mechanisms of *EMP3* in ccRCC, GSEA was used to explore the enrichment signaling pathways and possible biological functions of *EMP3*. As shown in Fig. 7A, fatty acid metabolism was inhibited. Previously, we documented that lipid consumption could inhibit the malignant phenotypes of ccRCC cells [21, 22]. Accordingly, oil red staining and triglyceride determination were performed in the present study to validate that knockdown of *EMP3* could reduce intracellular lipid accumulation (Fig. 7B,C). GSEA revealed that *EMP3* was significantly enriched in Epithelial-mesenchymal transition (EMT) and Myc Targets V2 signaling pathways. The correlation plot of gene expression demonstrated that *EMP3* was negatively correlated with E-cadherin (CDH1) and positively correlated with VIM, SNAIL and N-cadherin (CDH2), which were confirmed by Western blot (Fig. 7D,E). The above findings indicated that *EMP3* could increase tumor malignancy by promoting EMT and lipid accumulation in ccRCC.

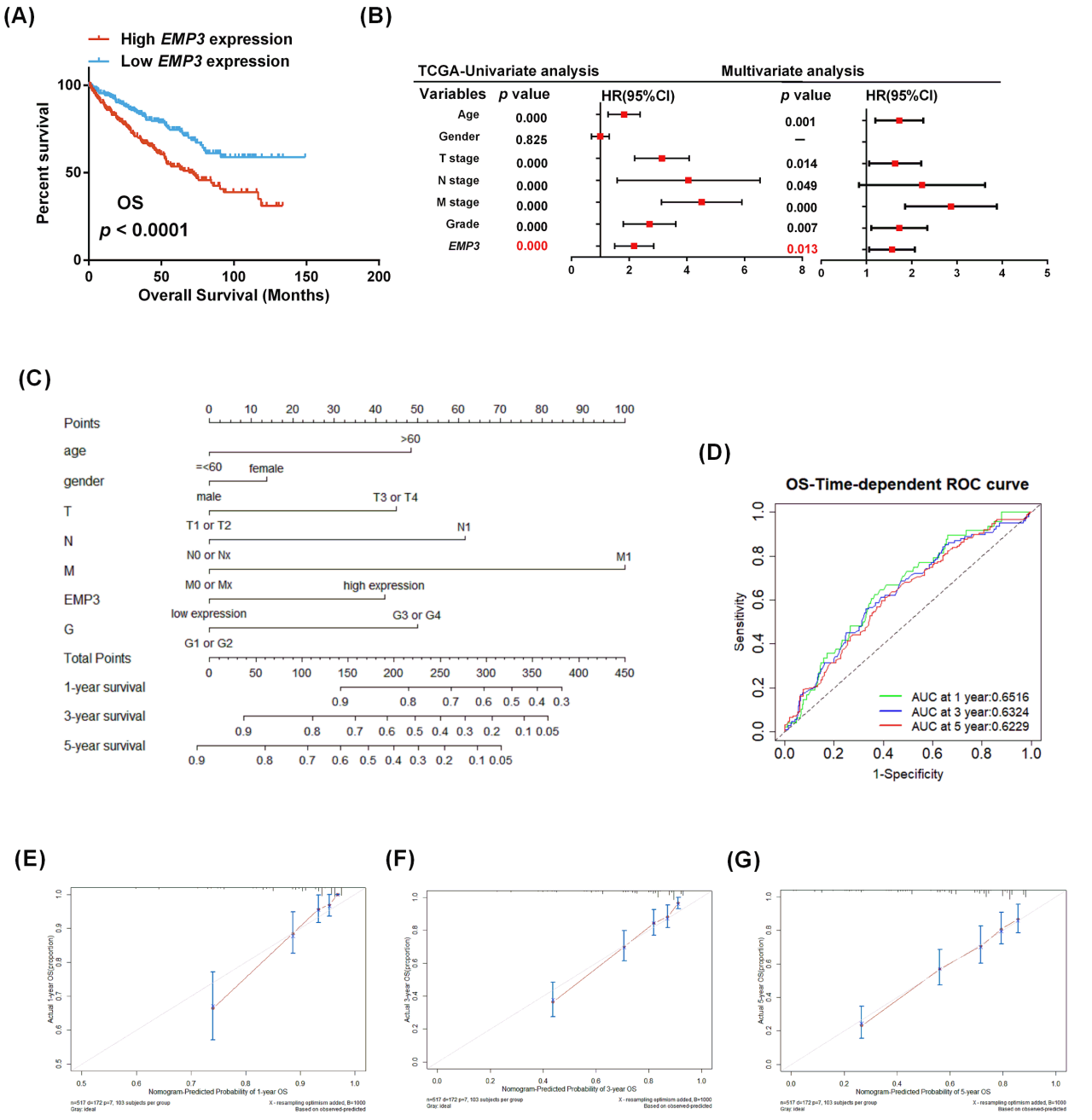

Fig. 4. *EMP3* is a biomarker of ccRCC with prognostic significance. (A) Kaplan-Meier curves showed that different expression levels of *EMP3* were related to overall survival (OS) of ccRCC patients. (B) Univariate and multivariate analyses between *EMP3* mRNA level and overall survival of ccRCC patients. (C) The nomogram for predicting the probability of 1-, 3-, and 5-year overall survival in ccRCC patients. (D) The time-dependent ROC curves of 1-, 3-, and 5-year overall survival probabilities for ccRCC patients were predicted by nomogram. (E–G) The calibration curves of overall survival probabilities of 1-, 3-, and 5-year were predicted by nomogram in ccRCC patients.

4.8 The expression pattern of *EMP3* is related to tumor immune characteristics in ccRCC

The TIMER 2.0 online tool was used to explore the relationship between *EMP3* expression pattern and tumor immune infiltration in ccRCC. The results in **Supplementary Fig. 4** showed that the expression of *EMP3* had a significant correlation with a variety of immune cells, including $CD8^+$ T cells ($p = 3.04 \times 10^{-6}$, Rho = 0.215), macrophages ($p = 1.86 \times 10^{-3}$, Rho = –0.145), neutrophils ($p = 1.49 \times 10^{-2}$, Rho = 0.113) and myeloid dendritic cells ($p = 2.10 \times 10^{-11}$, Rho = 0.305), which also had a significant negative correlation with tumor purity in KIRC ($p = 4.67 \times 10^{-6}$, Rho = –0.211). However, there was no significant correlation observed in $CD4^+$ T cells and B cells ($p < 0.05$).

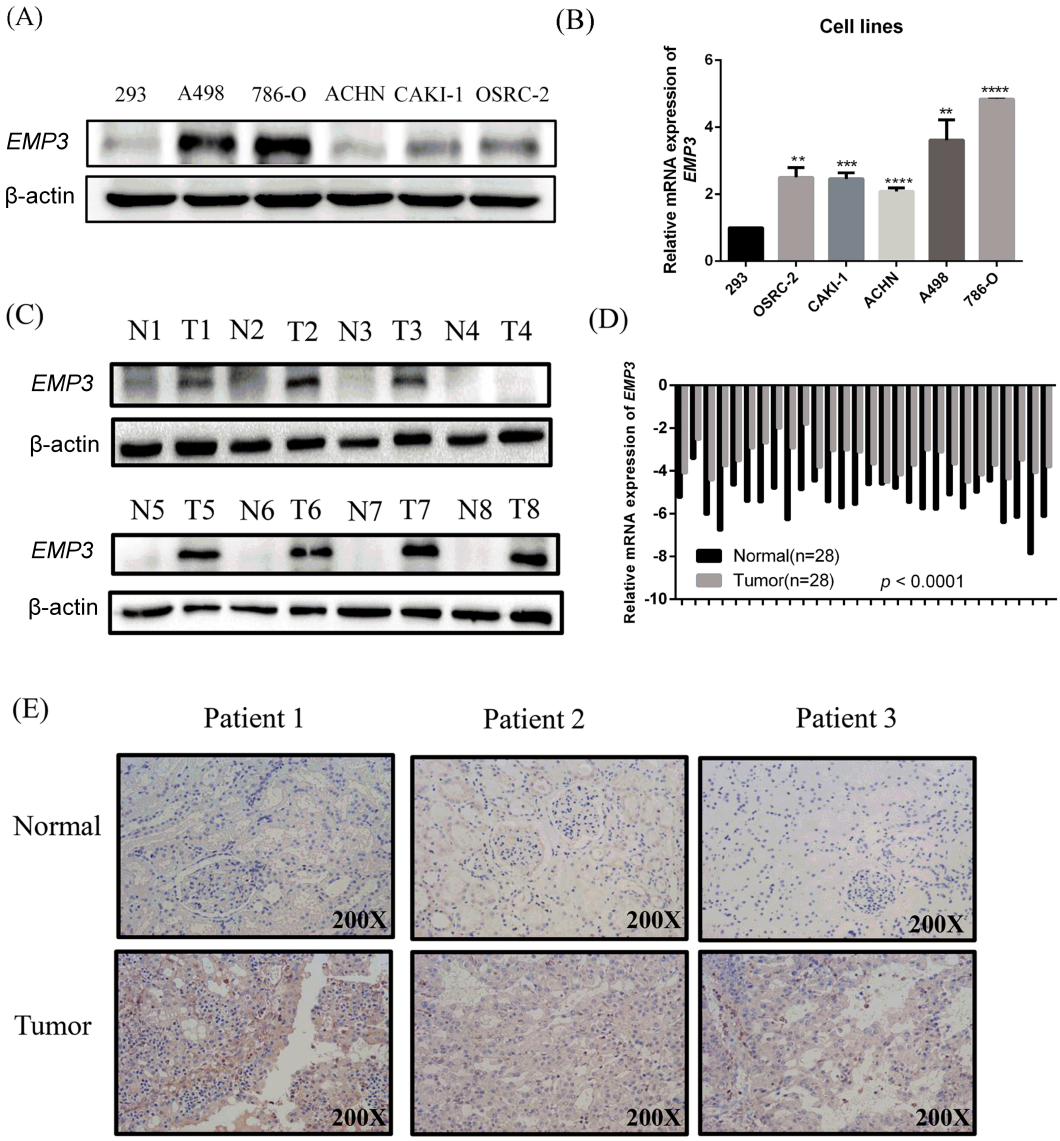

Fig. 5. *EMP3* is significantly upregulated in ccRCC cell lines and tissues. The expression of *EMP3* in ccRCC clinical samples and cell lines. (A,B) Analysis of *EMP3* expression in ccRCC cell lines using Western blot and qRT-PCR. (C–E) Verification of *EMP3* expression in clinical tissues using qRT-PCR, Western blot and IHC. *$p < 0.05$; **$p < 0.01$; ***$p < 0.001$; ****$p < 0.0001$.

Given that *EMP3* expression was closely related to several immune cells, we focused on several characteristic immune checkpoints, including CD274 ($p = 5.37 \times 10^{-5}$, Rho = –0.174), PDCD1 ($p = 1.69 \times 10^{-16}$, Rho = 0.347), CTLA4 ($p = 8.83 \times 10^{-11}$, Rho = 0.276), LAG3 ($p = 2.54 \times 10^{-21}$, Rho = 0.395), CD160 ($p = 1.21 \times 10^{-1}$, Rho = 0.067) and IDO2 ($p = 1.24 \times 10^{-2}$, Rho = 0.108). The results suggested that the up-regulated *EMP3* in ccRCC may be closely related to T cell exhaustion, thereby promoting tumor immune escape.

5. Discussion

With in-depth research on the pathophysiological mechanism of advanced ccRCC in the past few decades, its clinical treatment strategies have gradually enriched, including anti-angiogenic drugs, multi-kinase inhibitors, and immune checkpoint inhibitors (ICI) [23–26]. However, the 5-year survival rate of nonlocalized ccRCC patients followed up was only 10.5% according to a multicenter experience [27]. Currently, most of the constructed prognostic models for cancer patients were achieved by integrating multiple effective biomarkers, which could predict the survival outcomes of patients more accurately and personally [28–30]. Therefore, it will greatly benefit ccRCC patients to find novel and effective biomarkers.

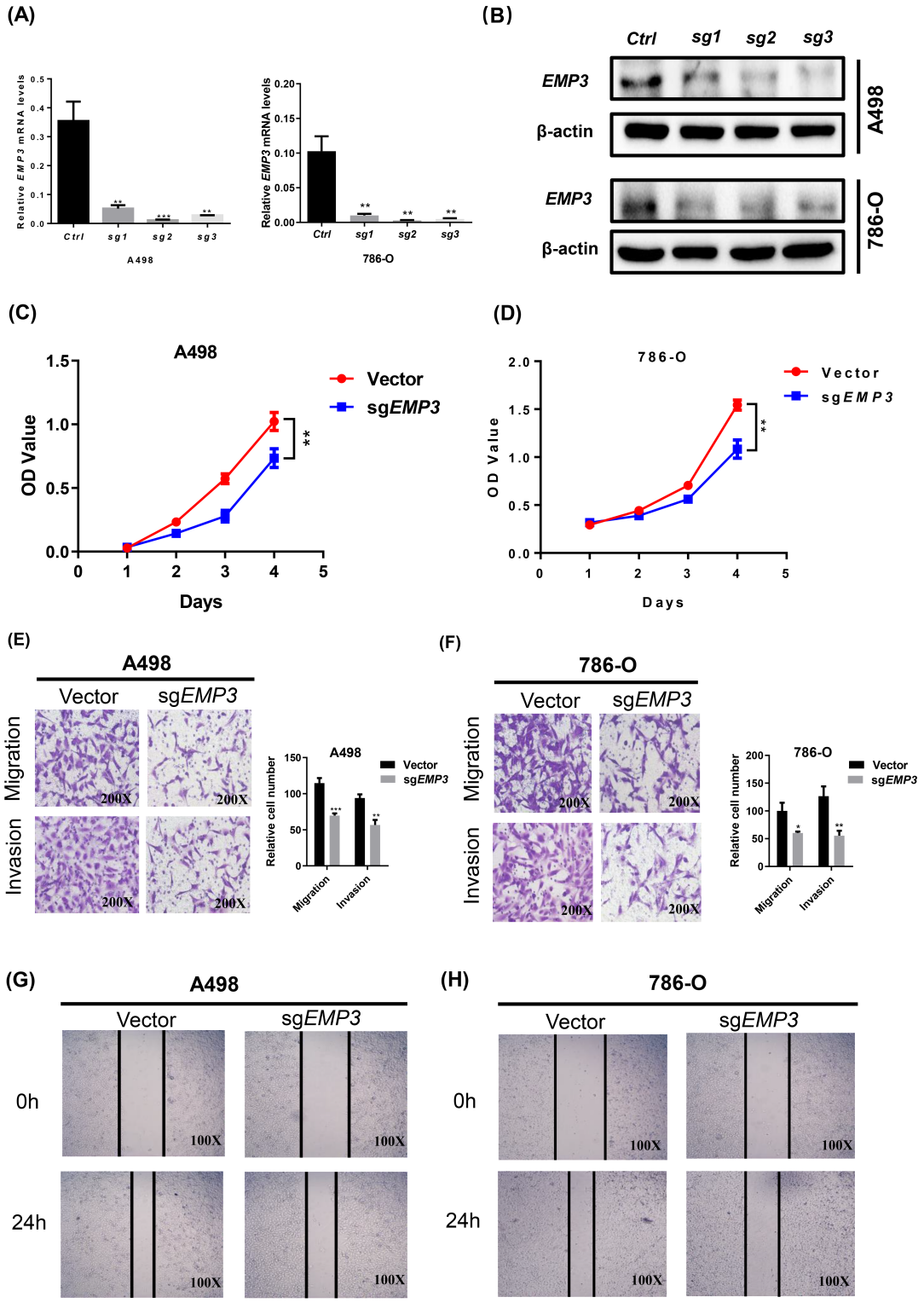

Fig. 6. Knockdown of *EMP3* inhibits the malignant phenotypes of ccRCC *in vitro*. (A,B) The expressions of *EMP3* mRNA and protein were successfully knockdown in A498 and 786-O cells. (C,D) CCK-8 assays showing cell growth curves of A498 and 786-O cells. (E,F) Representative images of migration and invasion assays performed using A498 and 786-O cells; the number of cells was counted in five randomly selected images from each group. (G,H) Wound healing of *EMP3*-knockdown A498 and 786-O cells at 0 hour and 24 hours (scale bar =200 μm). *$p < 0.05$; **$p < 0.01$; ***$p < 0.001$; ****$p < 0.0001$.

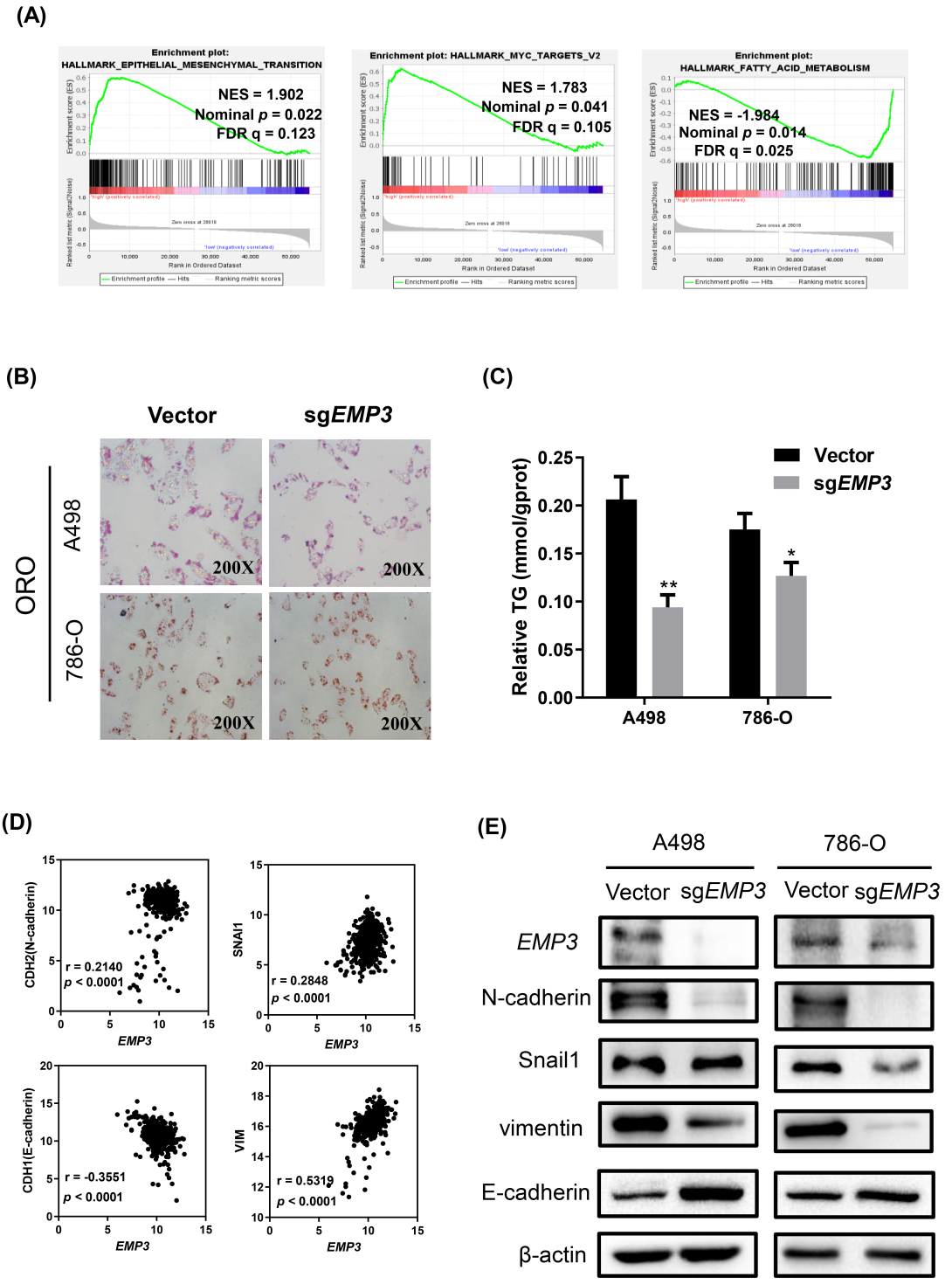

Fig. 7. *EMP3* affects the malignant phenotypes of ccRCC by promoting EMT and lipid accumulation. (A) GSEA was performed to investigate the biological pathways that may be involved in the regulation of *EMP3* based on the TCGA database. (B,C) Photomicrographs of Oil Red O staining of knockdown *EMP3* cell lines and its negative control (Magnification: 200 ×, scale bar = 50 μm). Relative TG (mmol/gprot) detected by triglyceride assay kit. (D) The correlations of E-cadherin, VIM, SNAIL and N-cadherin and *EMP3* were performed using the TCGA-KIRC data. (E) These related EMT markers were tested by Western blot after knockdown of *EMP3*. *$p < 0.05$; **$p < 0.01$.

EMP3, an epithelial membrane protein that regulates diverse membrane functions, has been reported to be a promising biomarker for ccRCC. Multi-database mining found that *EMP3* was significantly upregulated in ccRCC. Herein, we expounded the relationship between various clinicopathological parameters and the *EMP3* expression.

Using the TCGA-KIRC dataset, *EMP3* expression was found to be positively correlated with pathological grading and tumor staging. Besides, univariate and multivariate analysis showed that *EMP3* expression was an independent risk factor of OS in ccRCC patients. Furthermore, functional experiments showed that the malignant phenotype of tumor cells, including proliferation, migration, invasion, was significantly inhibited after knocking down *EMP3 in vitro*. Mechanistically, *EMP3* expression knockdown suppressed the malignant behavior of renal cancer cells via regulation of the EMT process and intracellular lipid degradation. Overall, our findings uncovered that *EMP3* might be an oncogene that could be harnessed to predict poor prognosis in ccRCC patients.

An increasing body of evidence suggests that epithelial membrane protein family members are involved in tumor progression and metastasis. Previous reports revealed that the expression patterns of EMPs were dysregulated in various human malignancies [31, 32]. Liu *et al*. [33] found that *in vitro* EMP1 could enhance the malignant phenotypes of ovarian cancer via the MAPK signaling pathway. Similarly, *EMP3* has been reported to be a candidate tumor-promoting gene in many types of tumors, including gastric cancer (GC), breast carcinoma and glioblastoma (GBM). Guo *et al*. [34] speculated that *EMP3* could be a downstream target of CD13 and played a crucial role in the PI3K/AKT pathway, promoting EMT and cisplatin resistance in gastric cancer (GC) cells. In addition, *EMP3* reportedly behaved as an oncogene in breast cancer and correlated with a more aggressive phenotype [35]. Interestingly, previous experimental results uncovered that *EMP3* could enhance M2 tumor-associated macrophages (TAMs) infiltration and restrained intratumoral $CD4^+$ and $CD8^+$ T cell infiltration in glioblastoma (GBM), resulting in immune escape to facilitate tumor progression [36]. However, to the best of our knowledge, there is the first study to document the role of *EMP3* in ccRCC. We hypothesized that *EMP3* could mediate the malignant phenotype of ccRCC tumor cells. Analysis of the expression levels, diagnostic value, prognostic role and underlying mechanisms of *EMP3* in ccRCC showed that *EMP3* promoted the EMT process and inhibited fatty acid degradation in cancer cells. Importantly, *EMP3* could act as a promising biomarker to assist diagnosis and predict the survival of ccRCC patients.

Epithelial-mesenchymal transition is characterized by cell transdifferentiation that loosens cell adhesion, confers enhanced invasiveness to cells, and is closely related to advanced tumor metastasis [37]. The loss of epithelial characteristics and the improvement of mesenchymal activity can reportedly empower cancer cells with stronger abilities to survive and spread [38, 39]. Meanwhile, many related EMT-activating transcription factors, including SNAIL, ZEB1 and TWIST1, have been documented with corresponding regulatory alterations, which mediate the EMT process largely [40, 41]. According to reports in the literature, *EMP3* as a target gene is regulated by a variety of microRNAs and affects the progression of malignant tumors [11, 42]. Our previous research showed that miR-765 was down-regulated in ccRCC and could alleviate tumor progression by eliminating lipids [21]. As a potential upstream molecule of *EMP3*, miR-765 can inhibit its expression and prevent the metastasis of cancer cells, and it is worth noting that the EMT process may be involved [42–44]. The results indicated that *EMP3* had a positive relationship with EMT-activating transcription factors and mesenchymal markers; however, it negatively correlated with epithelial marker E-cadherin. Based on our study findings, we can infer that *EMP3* can promote the malignant phenotypes of ccRCC through the EMT process. However, deciphering the specific mechanism underlying this process warrants further studies.

Reprogramming of fatty acid metabolism is an important feature of kidney cancer [45]. The accumulation of "lipid droplets" in the cytoplasm is regarded as a hallmark of ccRCC, which is conducive to the survival and growth of cancer cells. As previously described, redundant lipid droplets are consumed in ccRCC through PLCL1/UCP1-mediated lipid browning to achieve the purpose of inhibiting tumor progression [46]. Accordingly, reducing lipid deposition and storage in ccRCC could have huge prospects as a novel therapeutic approach. Furthermore, in the present study, we documented that *EMP3* knockdown could significantly alleviate the burden of lipid storage in ccRCC cancer cells. However, the mechanism underlying the regulation of lipid metabolism by *EMP3* in ccRCC remains largely unexplored, requiring further in-depth investigation.

In recent years, the dysregulation of the immune microenvironment in cancer has become a research hotspot worldwide. The relationship between *EMP3* expression and tumor immune should be explored, which can not only better explain the reasons for ccRCC deterioration, but also provide new ideas for subsequent in-depth research. Through the analysis of immune cell infiltration in the tissues of 533 KIRC patients based on the TIMER2.0 database, we found that the expression of *EMP3* had a positive relationship with $CD8^+$ T cells, neutrophils and myeloid dendritic cells. Further genes co-expression analysis found that *EMP3* was significantly positively correlated with a variety of characteristic immune checkpoints, including PDCD1, CTLA4, LAG3 and IDO2. These results implied that *EMP3*'s role as a carcinogen in ccRCC may be related to T cell exhaustion, resulting in tumor immune escape. It was reported that the programmed death ligand-1/programmed death-1 (PD-L1/PD-1) was a vital component of tumor immunosuppression [47, 48]. Therefore, it may explain the phenomenon that parts of advanced KIRC patients had a significant therapeutic effect after using ICIs, which greatly prolonged their life expectancy.

6. Conclusions

Herein, by combining bioinformatics analysis and experiments, we revealed that *EMP3* was highly expressed and correlated with poor overall survival in ccRCC. Moreover, we showed that *EMP3* could act as an oncogene related to immune infiltration, EMT process and lipid accumulation in ccRCC. In light of our findings, we believe that detecting *EMP3* as a novel biomarker may have broad prospects to diagnose and treat patients with ccRCC early, thereby improving the tumor prognosis.

7. Author contributions

QL, WX, and ZX designed and carried out all the experiments involved in the research. JS, DM, XM and HY (Hongwei Yuan) performed the statistical analysis and participated in the collection of clinical samples. HY (Hongmei Yang) edited the paper and XZ revised the paper. All authors read and approved the manuscript. All authors reviewed the paper and approved the final manuscript.

8. Ethics approval and consent to participate

The authors are accountable for all aspects of the work in ensuring that questions related to the accuracy or integrity of any part of the work are appropriately investigated and resolved. All procedures performed in studies involving human participants were in accordance with the ethical standards of the Institutional Review Board of Huazhong University of Science and Technology (S175).

9. Acknowledgment

Thanks to all the peer reviewers for their opinions and suggestions. Data were publicly accessible which can be obtained in The Cancer Genome Atlas (TCGA) and Oncomine databases. Thanks for the support of these public databases.

10. Funding

This study was supported by the National Key Scientific Instrument Development Project (81927807), National Key R&D Program of China (2017YFB1303100), Wuhan Science and Technology Plan Application Foundation Frontier Project (2020020601012247), Technology and Innovation Commission of Shenzhen Municipality (JCYJ20190809102415054), and the National Natural Scientific Foundation of China (Grant NO. 81902588).

11. Conflict of interest

These authors declare no conflict of interest.

12. References

[1] Sung H, Ferlay J, Siegel RL, Laversanne M, Soerjomataram I, Jemal A, *et al*. Global Cancer Statistics 2020: GLOBOCAN Estimates of Incidence and Mortality Worldwide for 36 Cancers in 185 Countries. CA-A Cancer Journal for Clinicians. 2021; 71: 209–249.

[2] Hsieh JJ, Purdue MP, Signoretti S, Swanton C, Albiges L, Schmidinger M, *et al*. Renal cell carcinoma. Nature Reviews Disease Primers. 2017; 3: 17009.

[3] Ljungberg B, Albiges L, Abu-Ghanem Y, Bensalah K, Dabestani S, Fernández-Pello S, *et al*. European Association of Urology Guidelines on Renal Cell Carcinoma: the 2019 Update. European Urology Oncology. 2019; 75: 799–810.

[4] Cohen HT, McGovern FJ. Renal-Cell Carcinoma. New England Journal of Medicine. 2005; 353: 2477–2490.

[5] Motzer RJ. Perspective: what next for treatment? Nature. 2016; 537: S111.

[6] Taylor V, Suter U. Epithelial membrane protein-2 and epithelial membrane protein-3: two novel members of the peripheral myelin protein 22 gene family. Gene. 1996; 175: 115–120.

[7] Wilson HL, Wilson SA, Surprenant A, North RA. Epithelial membrane proteins induce membrane blebbing and interact with the P2X7 receptor C terminus. The Journal of Biological Chemistry. 2002; 277: 34017–34023.

[8] Huang RY, Kuay KT, Tan TZ, Asad M, Tang HM, Ng AHC, *et al*. Functional relevance of a six mesenchymal gene signature in epithelial-mesenchymal transition (EMT) reversal by the triple angiokinase inhibitor, nintedanib (BIBF1120). Oncotarget. 2016; 6: 22098–22113.

[9] Fumoto S, Tanimoto K, Hiyama E, Noguchi T, Nishiyama M, Hiyama K. *EMP3*as a candidate tumor suppressor gene for solid tumors. Expert Opinion on Therapeutic Targets. 2009; 13: 811–822.

[10] Xue Q, Zhou Y, Wan C, Lv L, Chen B, Cao X, *et al*. Epithelial membrane protein 3 is frequently shown as promoter methylation and functions as a tumor suppressor gene in non-small cell lung cancer. Experimental and Molecular Pathology. 2014; 95: 313–318.

[11] Ma Q, Zhang Y, Liang H, Zhang F, Liu F, Chen S, *et al*. *EMP3*, which is regulated by miR-663a, suppresses gallbladder cancer progression via interference with the MAPK/ERK pathway. Cancer Letters. 2019; 430: 97–108.

[12] Kunitz A, Wolter M, van den Boom J, Felsberg J, Tews B, Hahn M, *et al*. DNA hypermethylation and aberrant expression of the *EMP3* gene at 19q13.3 in Human Gliomas. Brain Pathology. 2007; 17: 363–370.

[13] Alaminos M, Dávalos V, Ropero S, Setién F, Paz MF, Herranz M, *et al*. *EMP3*, a myelin-related gene located in the critical 19q13.3 region, is epigenetically silenced and exhibits features of a candidate tumor suppressor in glioma and neuroblastoma. Cancer Research. 2005; 65: 2565–2571.

[14] Han M, Xu W. *EMP3* is induced by TWIST1/2 and regulates epithelial-to-mesenchymal transition of gastric cancer cells. Tumour Biology. 2017; 39: 1010428317718404.

[15] Wang Y, Li W, Wu W, Chai C, Liu H, Lai M, *et al*. Potential significance of *EMP3* in patients with upper urinary tract urothelial carcinoma: crosstalk with ErbB2-PI3K-Akt pathway. The Journal of Urology. 2015; 192: 242–251.

[16] Liu J, Lichtenberg T, Hoadley KA, Poisson LM, Lazar AJ, Cherniack AD, *et al*. An Integrated TCGA Pan-Cancer Clinical Data Resource to Drive High-Quality Survival Outcome Analytics. Cell. 2018; 173: 400–416.e411.

[17] Sanchez-Vega F, Mina M, Armenia J, Chatila WK, Luna A, La KC, *et al*. Oncogenic Signaling Pathways in the Cancer Genome Atlas. Cell. 2019; 173: 321–337.e10.

[18] Rhodes DR, Yu J, Shanker K, Deshpande N, Varambally R, Ghosh D, *et al*. ONCOMINE: a cancer microarray database and integrated data-mining platform. Neoplasia. 2004; 6: 1–6.

[19] Sarkans U, Füllgrabe A, Ali A, Athar A, Behrangi E, Diaz N, *et al*. From ArrayExpress to BioStudies. Nucleic Acids Research. 2021; 49: D1502–D1506.
[20] Li T, Fu J, Zeng Z, Cohen D, Li J, Chen Q, *et al*. TIMER2.0 for analysis of tumor-infiltrating immune cells. Nucleic Acids Research. 2020; 48: W509–W514.
[21] Xiao W, Wang C, Chen K, Wang T, Xing J, Zhang X, *et al*. MiR-765 functions as a tumour suppressor and eliminates lipids in clear cell renal cell carcinoma by downregulating PLP2. EBioMedicine. 2020; 51: 102622.
[22] Xiao W, Wang X, Wang T, Chen B, Xing J. HAO2 inhibits malignancy of clear cell renal cell carcinoma by promoting lipid catabolic process. Journal of Cellular Physiology. 2019; 234: 23005–23016.
[23] Atkins MB, Tannir NM. Current and emerging therapies for first-line treatment of metastatic clear cell renal cell carcinoma. Cancer Treatment Reviews. 2018; 70: 127–137.
[24] Gul A, Stewart TF, Mantia CM, Shah NJ, Gatof ES, Long Y, *et al*. Salvage Ipilimumab and Nivolumab in Patients with Metastatic Renal Cell Carcinoma after Prior Immune Checkpoint Inhibitors. Journal of Clinical Oncology. 2020; 38: 3088–3094.
[25] Rini BI, Atkins MB. Resistance to targeted therapy in renal-cell carcinoma. The Lancet Oncology. 2009; 10: 992–1000.
[26] Briggs LG, Cone EB, Lee RJ, Blute ML. Prognostic and predictive biomarkers for metastatic renal cell carcinoma. Journal of Cancer Metastasis and Treatment. 2021; 7: 46.
[27] Patard J, Leray E, Rioux-Leclercq N, Cindolo L, Ficarra V, Zisman A, *et al*. Prognostic value of histologic subtypes in renal cell carcinoma: a multicenter experience. Journal of Clinical Oncology. 2005; 23: 2763–2771.
[28] Liu Z, Zhong J, Cai C, Lu J, Wu W, Zeng G. Immune-related biomarker risk score predicts prognosis in prostate cancer. Aging. 2020; 12: 22776–22793.
[29] Jeong S, Kim RB, Park SY, Park J, Jung E, Ju Y, *et al*. Nomogram for predicting gastric cancer recurrence using biomarker gene expression. European Journal of Surgical Oncology. 2020; 46: 195–201.
[30] Zhao E, Zhou C, Chen S. A signature of 14 immune-related gene pairs predicts overall survival in gastric cancer. Clinical and Translational Oncology. 2021; 23: 265–274.
[31] Wang Y, Cheng H, Ding Y, Chou L, Chow N. EMP1, EMP 2, and *EMP3* as novel therapeutic targets in human cancer. Biochimica Et Biophysica Acta. Reviews on Cancer. 2017; 1868: 199–211.
[32] Ahmat Amin MKB, Shimizu A, Ogita H. The Pivotal Roles of the Epithelial Membrane Protein Family in Cancer Invasiveness and Metastasis. Cancers. 2019; 11: 1620.
[33] Liu Y, Ding Y, Nie Y, Yang M. EMP1 Promotes the Proliferation and Invasion of Ovarian Cancer Cells Through Activating the MAPK Pathway. OncoTargets and therapy. 2020; 13: 2047–2055.
[34] Guo Q, Jing F, Xu W, Li X, Li X, Sun J, *et al*. Ubenimex induces autophagy inhibition and EMT suppression to overcome cisplatin resistance in GC cells by perturbing the CD13/*EMP3*/PI3K/AKT/NF-κB axis. Aging. 2019; 12: 80–105.
[35] Zhou W, Jiang Z, Li X, Xu F, Liu Y, Wen P, *et al*. *EMP3* Overexpression in Primary Breast Carcinomas is not Associated with Epigenetic Aberrations. Journal of Korean Medical Science. 2009; 24: 97.
[36] Chen Q, Jin J, Huang X, Wu F, Huang H, Zhan R. *EMP3* mediates glioblastoma-associated macrophage infiltration to drive T cell exclusion. Journal of Experimental & Clinical Cancer Research. 2021; 40: 160.
[37] Suarez-Carmona M, Lesage J, Cataldo D, Gilles C. EMT and inflammation: inseparable actors of cancer progression. Molecular Oncology. 2018; 11: 805–823.
[38] Hong X, Luo H, Zhu G, Guan X, Jia Y, Yu H, *et al*. SSR2 overexpression associates with tumorigenesis and metastasis of Hepatocellular Carcinoma through modulating EMT. Journal of Cancer. 2020; 11: 5578–5587.
[39] Mittal V. Epithelial Mesenchymal Transition in Tumor Metastasis. Annual Review of Pathology. 2018; 13: 395–412.
[40] Stemmler MP, Eccles RL, Brabletz S, Brabletz T. Non-redundant functions of EMT transcription factors. Nature Cell Biology. 2019; 21: 102–112.
[41] Sánchez-Tilló E, Liu Y, de Barrios O, Siles L, Fanlo L, Cuatrecasas M, *et al*. EMT-activating transcription factors in cancer: beyond EMT and tumor invasiveness. Cellular and Molecular Life Sciences. 2012; 69: 3429–3456.
[42] Zheng Z, Luan X, Zha J, Li Z, Wu L, Yan Y, *et al*. TNF-α inhibits the migration of oral squamous cancer cells mediated by miR-765-*EMP3*-p66Shc axis. Cellular Signalling. 2017; 34: 102–109.
[43] Hong XC, Fen YJ, Yan GC, Hong H, Yan CH, Bing LW, *et al*. Epithelial membrane protein 3 functions as an oncogene and is regulated by microRNA-765 in primary breast carcinoma. Molecular Medicine Reports. 2016; 12: 6445–6450.
[44] Kahm YJ, Kim RK, Jung U, Kim IG. Epithelial membrane protein 3 regulates lung cancer stem cells via the TGF-β signaling pathway. International Journal of Oncology. 2021; 59: 80.
[45] Wettersten HI, Hakimi AA, Morin D, Bianchi C, Johnstone ME, Donohoe DR, *et al*. Grade-Dependent Metabolic Reprogramming in Kidney Cancer Revealed by Combined Proteomics and Metabolomics Analysis. Cancer Research. 2015; 75: 2541–2552.
[46] Xiong Z, Xiao W, Bao L, Xiong W, Xiao H, Qu Y, *et al*. Tumor Cell "Slimming" Regulates Tumor Progression through PLCL1/UCP1-Mediated Lipid Browning. Advanced Science. 2019; 6: 1801862.
[47] Jiang X, Wang J, Deng X, Xiong F, Ge J, Xiang B, *et al*. Role of the tumor microenvironment in PD-L1/PD-1-mediated tumor immune escape. Molecular Cancer. 2019; 18: 10.
[48] Thompson RH, Dong H, Lohse CM, Leibovich BC, Blute ML, Cheville JC, *et al*. PD-1 is Expressed by Tumor-Infiltrating Immune Cells and is Associated with Poor Outcome for Patients with Renal Cell Carcinoma. Clinical Cancer Research. 2007; 13: 1757–1761.

Supplementary material: Supplementary material associated with this article can be found, in the online version, at https://www.fbscience.com/Landmark/articles/10.52586/5018.

Keywords: Epithelial membrane protein 3; ccRCC; Biomarker; EMT; Lipid accumulation; Immune infiltration

Send correspondence to:

Hongmei Yang, Department of Pathogenic Biology, School of Basic Medicine, Huazhong University of Science and Technology, 430022 Wuhan, Hubei, China, E-mail: hyang@hust.edu.cn

Xiaoping Zhang, Department of Urology, Union Hospital, Tongji Medical College, Huazhong University of Science and Technology, 430022 Wuhan, Hubei, China, Institute of Urology, Union Hospital, Tongji Medical College, Huazhong University of Science and Technology, 430022 Wuhan, Hubei, China, E-mail: xzhang@hust.edu.cn

† These authors contributed equally.